JACS
JOURNAL OF THE AMERICAN CHEMICAL SOCIETY
pubs.acs.org/JACS
Article

Target Profiling of an Iridium(III)-Based Immunogenic Cell Death Inducer Unveils the Engagement of Unfolded Protein Response Regulator BiP

Xiaolin Xiong,‖ Ke-Bin Huang,‖ Yuan Wang,‖ Bei Cao, Yunli Luo, Huowen Chen, Yan Yang, Yan Long, Moyi Liu, Albert S. C. Chan, Hong Liang,* and Taotao Zou*

Cite This: J. Am. Chem. Soc. 2022, 144, 10407−10416
Read Online

ABSTRACT: Clinical chemotherapeutic drugs have occasionally been observed to induce antitumor immune responses beyond the direct cytotoxicity. Such effects are coined as immunogenic cell death (ICD), representing a "second hit" from the host immune system to tumor cells. Although chemo-immunotherapy is highly promising, ICD inducers remain sparse with vague drug−target mechanisms. Here, we report an endoplasmic reticulum stress-inducing cyclometalated Ir(III)−bisNHC complex (**1a**) as a new ICD inducer, and based on this compound, a clickable photoaffinity probe was designed for target identification, which unveiled the engagement of the master regulator protein BiP (binding immunoglobulin protein)/GRP78 of the unfolded protein response pathway. This has been confirmed by a series of cellular and biochemical studies including fluorescence microscopy, cellular thermal shift assay, enzymatic assays, and so forth, showing the capability of **1a** for BiP destabilization. Notably, besides **1a**, the previously reported ICD inducers including KP1339, mitoxantrone, and oxaliplatin were also found to engage BiP interaction, suggesting the important role of BiP in eliciting anticancer immunity. We believe that the ICD-related target information in this work will help to understand the mode of action of ICD that is beneficial to designing new ICD agents with high specificity and improved efficacy.

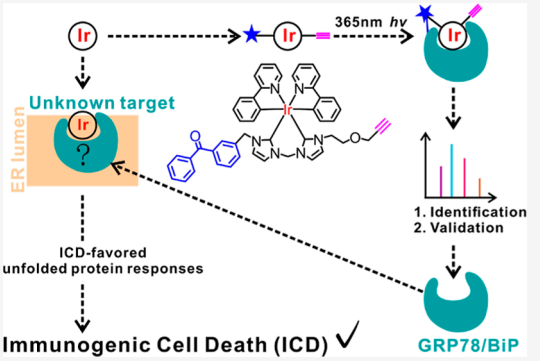

INTRODUCTION

Immunogenic cell death (ICD) is a unique response pattern of cell death that can provoke long-lasting antitumor immunity by inducing damage-associated molecular pattern (DAMP) signals such as surface exposure of calreticulin (CRT), release of ATP, and secretion of HMGB1.[1] For cancer cells, the released immunostimulatory signals during the ICD process lead to the enhanced engulfment of cancer cells by dendritic cells (DCs),[1] the most efficient antigen-presenting cells in the immune system.[2] Then, the cancer-specific antigens will be presented by DCs to the relevant T cells, resulting in the activation of a global anticancer immune response. After decades of endeavors, ICD was found inducible by diverse death types including necroptosis,[3] pyroptosis,[4] and some kinds of apoptosis.[5] Correspondingly, various ICD-inducing factors have been identified such as microbial components, irradiation, and particularly chemotherapy.[6]

Chemotherapeutic drugs with antitumor immunity can bring in a great bonus: a "first hit" by their cytotoxicity on the fast-growing cancer cells and a "second hit" from the host immune system to elicit tumor-specific immune responses.[7] Of note, studies have proven promising synergistic effects on the combined use of clinic-related ICD inducers (*e.g.*, oxaliplatin and doxorubicin) with PD-1/PD-L1 inhibitors.[8−10] A recent investigation also pointed out that the ICD agents, cyclophosphamide and oxaliplatin, powered CAR-T cells toward immunosuppressing solid tumors by altering the tumor microenvironment.[11] Related clinical trials are in process globally.[12,13] It is thus envisioned that ICD-based chemotherapy will play more important roles in immunotherapies in the future.

Beginning with doxorubicin, the first well-characterized ICD agent,[14] increasing examples were found to elicit ICD activities.[15,16] Of particular attention is the fast growth of metal-based ICD inducers in the past decade,[17,18] including the complexes of platinum,[19−30] ruthenium,[31−34] gold,[35,36] iridium,[37−39] manganese,[40] and copper.[41] While these compounds display intriguing antitumor immunity, the ICD response is usually tumor-type-limited, exemplified by the fact that oxaliplatin induced potent ICD in colorectal cancer

Received: March 4, 2022
Published: June 3, 2022

but failed in non-small cell lung cancer;[42] also, the structure–activity relationship for these ICD-provoking compounds appears unclear. In the literature, despite that endoplasmic reticulum (ER) stress is known as a prerequisite to eliciting ICD, not all ER stress could trigger immune responses.[43] In fact, the specific biotargets responsible for stimulating and maintaining the ICD-related ER stress are not yet well understood. Therefore, it is of urgent need in elucidating the mode of action of ICD at the molecular target level.

In this work, we aimed to understand the molecular mechanism of ICD based on a newly identified ICD inducer. In view of the fact that the constantly induced ER stress is a key feature of ICD, we examined a series of cyclometalated iridium(III) complexes and successfully unveiled the ICD activity of an ER-targeting Ir(III) complex (**1a**) containing a bis-*N*-heterocyclic carbene (bisNHC) ligand. The complex is capable of inducing all hallmarks of ICD and displays a vaccination effect similar to that of oxaliplatin in the mouse model. As the NHC ligand is easy to be functionalized, a homologue probe containing benzophenone and alkyne moieties was designed. The following target profiling and validation experiments emphasized the engagement of the binding immunoglobulin protein (BiP), a crucial protein that controls ER hemostasis with close relation to the ICD-resisting ability of the tumor. Further studies using clinic-related ICD agents suggested a universal engagement of the BiP target. To the best of our knowledge, it is the first time that the direct target information of ICD is obtained by a chemical biology approach, which, as we believe, will help to understand the molecular basis behind ICD and benefit the design of new inducers with better performance.

RESULTS AND DISCUSSION

Induction of ICD Activity by 1a. In the literature, the tight cross talk between ER stress and ICD has been proposed,[43] and many metal compounds were shown to be ER-targeting.[44] Our group also developed a platinum-amino-phosphonate-based ICD inducer with ER stress induction.[19] These clues lead us to evaluate the ICD potential of **1a**, an ER-localizing compound (Figure 1a).[45,46] To verify such potential, we picked HCT116 cells and its paralogue mouse-derived CT26 cells for the following assays.

We first performed fluorescence microscopy to check the subcellular localization of **1a** in HCT116 cells utilizing its intrinsic phosphorescence. As the images show (Figure 2a), the green emission of **1a** colocalized with ER Tracker Red with Pearson's correlation coefficient of 91%, calculated by Fiji software.[47] Such a result was consistent with a previous observation of **1a** in HeLa cells.[46] Next, we chose the immunofluorescence staining of cell surface-exposed CRT protein (ectoCRT) as a readout to check ICD activity, as ectoCRT is a dominant and early DAMP signal of ICD.[5,48,49] For comparison, three analogues **Ir-DMSO**, **Ir-NH$_2$**, and **Ir-bpy**, were examined as well (Figure 1a). We observed that **1a** treatment (12 μM, 3 h) led to a potent ectoCRT expression in HCT116 cells, but the other three complexes did not show similar activity (Figure 2b). The dose-dependent induction of ectoCRT by **1a** was then confirmed (Figure S1a). The other two markers, the increased ATP release and HMGB1 secretion, were also observed by **1a** treatment as anticipated (Figure S1b,c). In addition, the Ser51 site phosphorylation of eIF2α (P-eIF2α) was significantly boosted by **1a** in a dose-dependent manner (Figure S2), suggesting the possible global

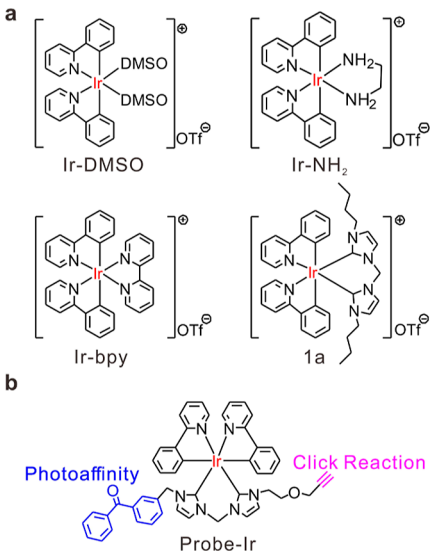

Figure 1. Chemical structures of Ir(III) complexes used in this study. (a) Examples of Ir(III) complexes for ectoCRT screening. (b) Photoaffinity probe of **1a** for target profiling.

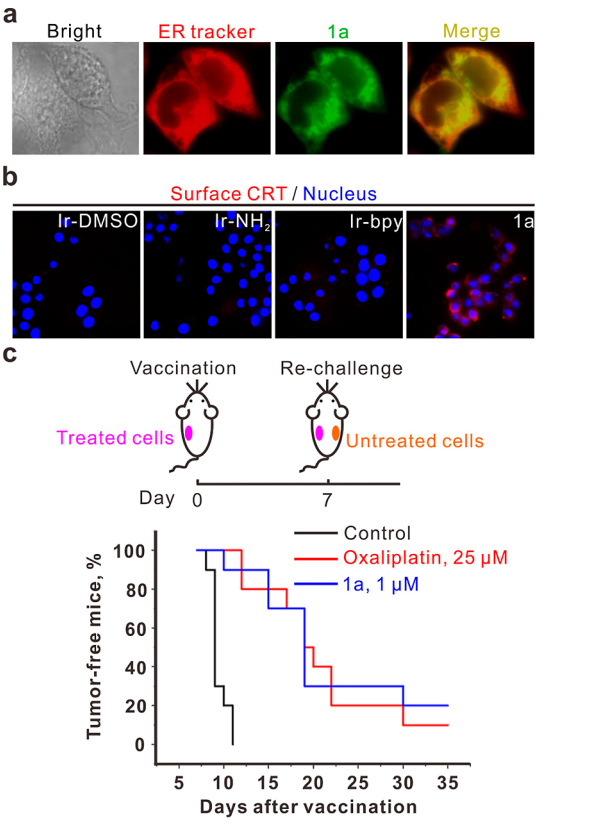

Figure 2. Induction of ICD by **1a**. (a) Subcellular localization of **1a**. HCT116 cells were stained by ER Tracker after **1a** treatment (12 μM, 15 min). The green fluorescence of **1a** was merged with the red signal of ER Tracker. (b) ectoCRT detection under the treatments of indicated Ir(III) complexes (12 μM, 3 h). (c) Mouse vaccination assay of **1a** using the mouse CT26 colon cancer cell line. Treated CT26 cells were injected into the left flank of the mouse. After 7 days, the untreated cells were injected into the right flank. The tumor-free mice percentage after rechallenging was shown at indicated treatments.

https://doi.org/10.1021/jacs.2c02435
J. Am. Chem. Soc. 2022, 144, 10407−10416

translation inhibition that has been identified as an ICD hallmark by varied chemotherapeutic agents.[50,51] In addition, the kinase responsible for such phosphorylation was irregularly located upon **1a** treatment (Figure S3), indicating a certain degree of dysfunction. All the biomarkers identified above implied that **1a** is a promising ICD candidate.

Then, a vaccination experiment on the mouse model, the gold standard assay for ICD evaluation,[52,53] was thereby performed. CT26 cells were first treated with **1a** (1 μM) or oxaliplatin (25 μM). The total administered amount of **1a** per mouse was no more than 0.7 mg/kg, far below its LD_{50} of 29 mg/kg (Figure S4). Then, the drug-treated cells were injected into the left side of the mice, and the same cell line (untreated) was rechallenged to the right flanks of the mouse body 7 days later. Subsequently, tumor formation in the right was examined every day (Figure 2c). Mice that did not carry the tumor in their right flanks were recorded as tumor-free mice. The percentage of tumor-free mice decreased to zero on the 11th day after rechallenging in the solvent group while retaining around 90% in the **1a**-treated group (Figure 2c). Tumor developments were delayed to a similar degree in **1a**- and oxaliplatin-treated groups. Thus, complex **1a** is truly an ICD inducer.

Development of a Clickable Photoaffinity Probe. After identifying **1a** as a new ICD agent, we sought to dig out its targets by developing a chemical biology probe for an advanced understanding of its mechanism. In this regard, benzophenone and alkyne were introduced on the bisNHC ligand for photoaffinity labeling and click reactions.[54−58] Initial attempts to make benzophenone- and alkyne-functionalized bis-imidazolium react with $[Ir(ppy)_2Cl]_2$ could not generate the desired products, possibly due to the high reactivity of the terminal alkyne. Then, we tried to prepare benzophenone- and hydroxyl-functionalized imidazolium and successfully obtained $[Ir(ppy)bisNHC^{-OH}]$ that was further reacted with 3-bromoprop-1-yne to generate **Probe-Ir** (Figure 1b) with a good yield. The detailed synthesis and characterization are shown in Supporting Information (Scheme S1 and Figures S5 and S6).

Target Profiling. Then, we examined whether the functionalization of benzophenone and alkyne moieties will influence the binding interactions of the Ir(III) complex with protein targets by using a competition assay. Briefly, the cells were treated with 10 μM of **Probe-Ir** with or without onefold **1a** for 2 h, followed by irradiation of 365 nm light for 15 min on ice. Then, the cells were lysed and the lysates were collected for the click reaction and streptavidin−horseradish peroxidase blotting. As shown in Figure S7a,b, the addition of **1a** successfully attenuated the blotting signals of **Probe-Ir**, suggesting that the modification does have little influence on the bindings of the parent compound. Then, we performed **Probe-Ir** treatment on living HCT116 cells, following similar cross-linking and labeling steps; then, the biotinylated proteomes were isolated by streptavidin pull-down assays. Subsequently, we performed the LC−MS/MS analysis on the enriched peptides to profile the targets (Figure 3a). Proteins not found in the control group while showing a high abundance in the probe treatment group were identified as the possible targets. Finally, 11 proteins were consistently found in repeated experiments (Table S1), which are mainly composed of ATP-related enzymes (such as BiP, HSPD1, and SLC25A4/SLC25A5) and protein chaperones (including P4HB, HSPD1, and BiP).

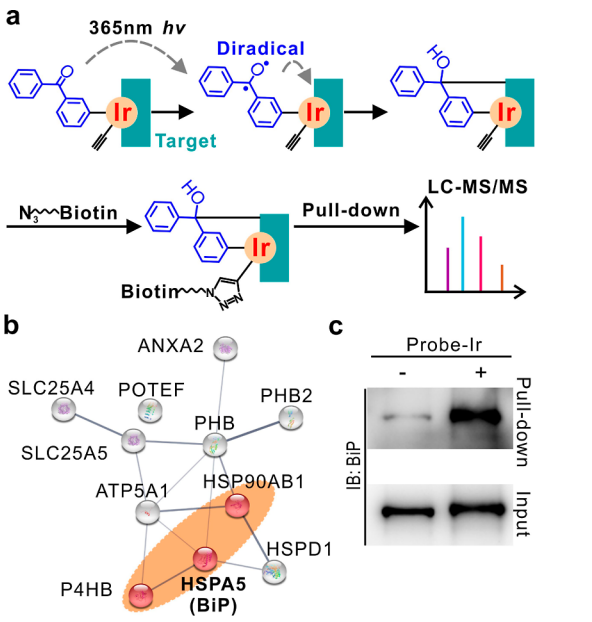

Figure 3. Target profiling using a **1a**-derived photoaffinity probe, **Probe-Ir**. (a) Workflow of target protein capturing and identification. (b) Protein association network was analyzed by a Web server STRING. The lines represent the experimentally verified interactions, and the thickness reflects the strength of the data support. Three protein dots that belong to "protein processing in ER" by the KEGG pathway analysis were labeled red and highlighted. (c) Pull-down western blot verification of BiP as the ER target of **Probe-Ir**. The "input" image indicated the BiP amount in the lysates.

As ER stress plays a vital role in ICD,[43] we applied the STRING analysis, an online server for mapping the protein association network,[59] to identify the ER-associated proteins. In the result shown in Figure 3b, three proteins−−P4HB (protein disulfide isomerase), BiP (also known as GRP78, 78 kDa glucose-regulated protein, or HSPA5), and HSP90AB1 (heat shock protein HSP90-β)−−were categorized into the "protein processing in ER" by the KEGG pathway analysis in STRING. In the literature, it is known that the chemical disturbance of proteostasis facilitates the occurrence of ICD *via* increased ER stress level. However, the outcome might differ because the following unfolded protein response (UPR) can lead to either cell death (ICD-favored) or stress adaptation (cell survival, ICD-unfavored).[60] In this regard, BiP has been known as the sole regulator of UPR by sensing the stress intensity and interacting with the whole three downstream pathways: PERK, IRE1, and ATF6.[61] Excessive unfolded protein over the BiP binding capacity is a key signal for proteotoxicity, constant ER stress, and defective cell adaptation.[62] Of the three ER-related proteins in our data, BiP also possesses a central role over other potential targets (Figure 3b). Based on the immunoblotting assay, BiP was successfully enriched in pull-down proteins by a BiP-specific antibody (Figure 3c). All prompted us to examine BiP in the following study.

Validation of BiP Targeting by 1a. In light of the emission property of **1a**, we conducted fluorescence microscopy to evaluate its colocalization with BiP. HCT116 cells were transiently transfected with a BiP−mCherry plasmid expressing the mCherry-fused BiP protein with red emission,[63] followed by **1a** treatment for a short time (15 min). Results showed that the green emission from **1a** was found to be

https://doi.org/10.1021/jacs.2c02435
J. Am. Chem. Soc. 2022, 144, 10407−10416

largely overlaid with the red signal of the fused proteins (Figure 4a), suggestive of good colocalization in living cells (Pearson's correlation coefficient at 89%).

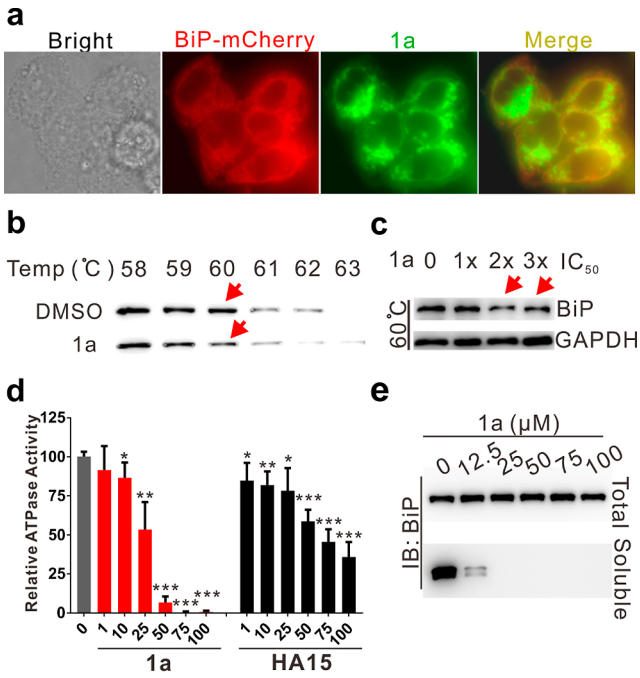

Figure 4. Validation of BiP engagement with **1a**. (a) Colocalization of BiP and **1a**. HCT116 cells were transfected with BiP−mCherry plasmid to overexpress the fluorescence-labeled BiP. (b) Western blot image of CETSA of BiP under the indicated temperatures. (c) ITDR assay in HCT116 cells at 60 °C of BiP under **1a** treatment. GAPDH protein was detected as a loading control. (d) ATPase activity of BiP upon the indicated concentrations of **1a** or HA15. Data represent mean ± SD (unpaired two-sided Student's *t* test; $n = 3$ total data points from three independent experiments). $^{*}p < 0.05$, $^{**}p < 0.01$, $^{***}p < 0.001$. (e) **1a**-induced solubility reduction of BiP. The soluble fractions represent the soluble BiP in the supernatant after centrifugation. 0.25 μM BiP was used for each incubation, with the indicated concentrations of **1a**. The samples of "total" were acquired without centrifugation.

Then, we conducted the cellular thermal shift assay (CETSA).[64] The change of thermal stability of proteins could reveal the binding interactions by either enhancing[58,65] or destabilizing[66,67] the thermal stability of target proteins. In our case, HCT116 cells were treated with 2× IC_{50} of **1a**, and then the freeze−thaw lysate was heated at the indicated temperatures, followed by centrifugation to remove the insoluble fraction, leaving the soluble ones for immunoblotting. As depicted in Figure 4b, **1a** significantly destabilized BiP at ∼60 °C. In the meantime, the isothermal dose−response (ITDR) assay by treating HCT116 cells with different concentrations of **1a** at a fixed 60 °C was also performed, showing a dose-dependent destabilization of BiP by **1a** treatment (Figure 4c). ITDR results also indicated the selectivity of **1a** toward BiP, compared with GAPDH. These results indicated that **1a** intracellularly binds to and destabilizes BiP.

Next, we investigated the BiP−**1a** engagement at the biochemical level by measuring the ATPase activity of the recombinant BiP. Such activity is generated by the nucleotide-binding domain of BiP and plays a vital role in the allosteric cycles of its binding to client or signal proteins.[68,69] As expected, **1a** dramatically dampened the ATPase activity of BiP (Figure 4d) at concentrations >10 μM. The inhibition ability of **1a** is much stronger than the known BiP inhibitor HA15[70] at the same concentrations (Figure 4d). Interestingly, at a low concentration (<10 μM), **1a** conferred weak inhibitory effects toward BiP that is similar to HA15.

However, a dramatic decrease in ATP hydrolysis was seen when the concentration of **1a** was over 10 μM. Complete suppression was found at 75 μM of **1a**, while HA15 at 100 μM only resulted in an inhibition of less than 70%. Together with the CETSA data which indicated BiP destabilization, we then checked the integrity of BiP. After **1a** treatment, a part of the sample was centrifuged to remove the insoluble protein pellet, while the uncentrifuged portion reflects the integrity of BiP. The centrifuge condition was set equal to that used in CETSA. Interestingly, **1a** did not alter the total BiP amount or induce shearing bands reflecting degradation. Instead, a large reduction of its soluble form was observed (Figure 4e) from 12.5 to 100 μM of **1a** treatment, indicating the formation of insoluble proteins. The dose-dependent behavior was similar to that of the former ATPase assays. In addition, the result based on native polyacrylamide gel electrophoresis (PAGE) gels was in support of the observations above. Upon **1a** treatment, denatured BiP failed to run into the gels, suggesting protein aggregation that is possibly caused by **1a**-induced BiP destabilization (Figure S8). Then, the binding affinity of **1a** was estimated by measuring the tryptophan fluorescence (ex: 280 nm; em: 350 nm). The dissociation constant (K_D) of **1a** was calculated to be 5.6×10^{-7} M (Figure S9), indicating a strong interaction at the submicromolar level. Taken together, **1a** deactivated BiP activity by direct binding and destabilization.

BiP Engagement by Other ICD Inducers. To examine if BiP is generally engaged in ICD, we attempted to test other ICD agents. So far, the only connection between ICD and BiP inhibition is a ruthenium-based KP1339 (also known as IT-139), a clinic drug candidate[71] that was known to down-regulate BiP expression[72] and induce ER stress and apoptosis.[73,74] A recent study also unveiled its ICD activity in the HCT116 colon cancer cell line,[31] but no direct BiP−KP1339 relationship was suggested.[75] The target profiling using KP1339−human serum albumin revealed the engagement of a transcription regulator that controls the BiP expression.[75] The lack of evidence for direct interaction drove us to check its inhibitory effect on the enzymatic activity of BiP. As shown in Figure 5a, at the same 100 μM concentration, KP1339 suppressed the ATP hydrolysis of BiP by a degree slightly lower than **1a** while still much higher than HA15 (Figure 5a). Next, we evaluated the solubility of BiP, revealing that KP1339 also induced BiP aggregation (Figure 5b). Thus, in addition to the previously reported suppression of BiP at the transcriptional level, our data suggested that KP1339 can also confer a direct targeting toward BiP in a way similar to **1a**.

In addition to KP1339, we chose mitoxantrone (MTX) and oxaliplatin (OXP) as the representatives of clinical ICD agents to check the commonality of BiP engagement. Nevertheless, the ATPase assay showed no inhibitory effect for MTX and a very weak effect for OXP (less than 30% inhibition) at 100 μM. Instead, CETSA curves revealed intracellular thermal shifts that occurred under MIX and OXP treatments for 2 h at their 2× IC_{50}, respectively (Figure 5c). The thermal stability

https://doi.org/10.1021/jacs.2c02435
J. Am. Chem. Soc. 2022, 144, 10407−10416

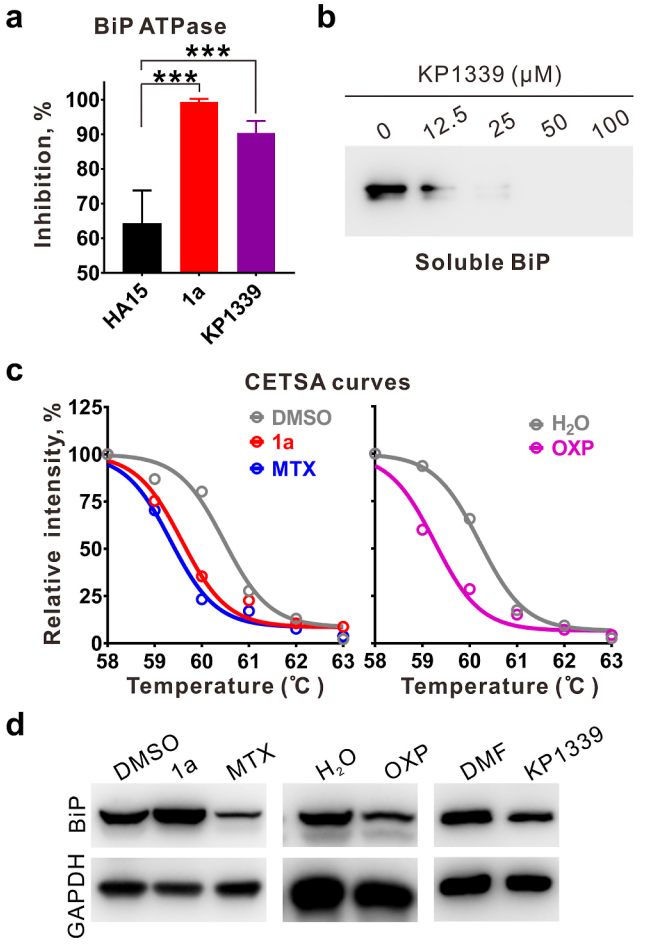

Figure 5. BiP association with other ICD-inducing agents. (a) KP1339 conferred inhibition on the BiP ATPase activity. The inhibition ratios were calculated by normalizing to the cognate solvent control of each compound. Data represent mean ± SD (unpaired two-sided Student's *t* test; data points from at least three independent experiments). Significance to the HA15 group was marked by asterisks, ***$p < 0.001$. (b) Solubility of BiP decreased upon KP1339 treatment. (c) CETSA curves comparing ICD agents MTX, OXP, and **1a**. The band intensity of the western blot at indicated temperatures was normalized to that at 58 °C. Each data point is the mean value of three independent assays. (d) Level of BiP in HCT116 cells under the indicated treatment. The image is representative of repeated experiments.

curves of MTX and OXP resembled that of **1a**, suggesting that BiP is directly destabilized in living cells. Importantly, ICD phenomena induced by MTX, OXP, KP1339, and **1a** all share the phosphorylation of eIF2α as a biomarker,[31,50] indicating the common activation of the ICD-promoting PERK branch after affecting BiP. In addition, we monitored the influence of each compound on BiP expression under 1× IC_{50} for 24 h (Figure 5d). As expected, KP1339 conferred a moderate downregulation as it can bind to a transcriptional factor responsible for BiP.[75] Of interest, MTX and OXP also lowered the amount of BiP. This may be caused by their ability to interfere with the genomic DNA metabolism and transcription.[76−79] Although the mechanism is unclear, simultaneously downregulating and destabilizing BiP may contribute to their efficacy in promoting ICD. In contrast, the BiP level upon **1a** treatment is slightly elevated, which is consistent with the literature report showing that BiP upregulation is a common sign of ER stress and UPR signaling,[80] indicating that **1a** targets BiP by directly destabilizing and inhibiting its activity rather than blocking the transcription or translation process. Overall, these observations indicated that ICD agents share BiP as a common target, albeit in different manners.

Role of BiP in Cancer and ICD. Since the role of BiP in ICD was identified, we sought to profile the BiP expression in cancers. The GEPIA2 Web server was applied for the analysis of the TCGA database.[81] First, we compared the expression of BiP in 33 types of cancer with their cognate normal tissues. Higher expressions were found, all in solid tumors occupying over one-third (13 out of 33) of the cancer types (Figures 6a

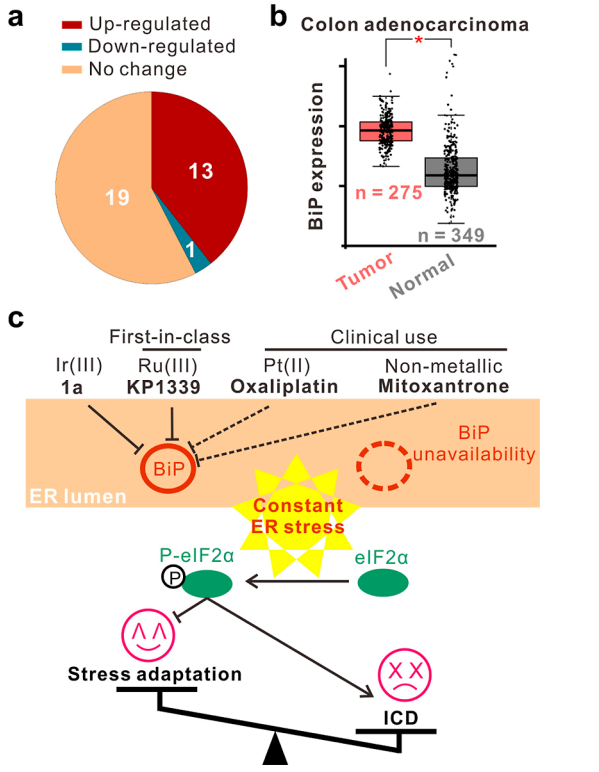

Figure 6. Role of BiP in cancers and ICD. (a) Pie chart of BiP mRNA expression in different tumors and cognate normal tissues. Thirty-three cancer types in total were taken into account based on the TCGA database. The groups with significantly higher and lower expressions of BiP in tumor versus normal tissues were labeled as red and cyan, respectively. Cancers with no significant changes in BiP expression were colored in light orange. (b) mRNA expression of BiP in colon adenocarcinoma. Data of tumor tissues were from TCGA while that of normal tissues were from TCGA and GTEx databases. The chart was generated by the GEPIA2 Web server. (c) Schematic graph of the discovery in this work.

and S10, exemplified by colon adenocarcinoma, and Figure 6b), with only one opposite situation in blood cancer. Next, we mapped the correlation of BiP expression with the overall survival in patients (Figure S11) using GEPIA2. In many cases, negative correlations were found, that is, the higher expression of BiP was associated with a bad survival rate in the case of adrenocortical carcinoma. Taken together, BiP is a highly promising tumor target. Overexpressed BiP in these cancer tissues might be a consequence of the enhanced ER stress caused by the aberrant protein synthesis.

Owing to its protective function, the higher expression of tumoral BiP has been linked to chemoresistance[82−84] and a

https://doi.org/10.1021/jacs.2c02435
J. Am. Chem. Soc. 2022, 144, 10407−10416

bad survival rate of patients.[85] Referring to ICD, a recent study claimed that glioma stem cells utilize BiP overexpression to avoid the irradiation-caused DAMP release.[86] Another research showed that ATAD3A protein could stabilize BiP to attenuate ER stress and compromise surface CRT exposure during oxaliplatin treatment in colon cancer cells.[87] The author also confirmed that a high BiP stability resulted in a weak anticancer immunity.[87] These studies suggested that ICD effects might be boosted by destabilizing or downregulating BiP, as proposed in Figure 6c.

CONCLUSIONS

In summary, we have identified a cyclometalated Ir(III) complex containing bisNHC ligand with potent ICD activity *in vitro* and *in vivo*. A clickable photoaffinity probe based on this ICD inducer unveiled a strong engagement of BiP targeting under cellular conditions. Further biochemical studies showed that the complex potently destabilized BiP, leading to the inhibition of the ATPase activity with much higher potency than the literature-reported inhibitor HA15. Additional studies by other clinic-related ICD inducers suggest a general BiP engagement by direct protein binding and/or expression inhibition.

Compounds that robustly disrupt ER homeostasis are likely to elicit a potent DAMP release.[88,89] With the BiP targeting identified here, new ICD compounds may be designed with the BiP-suppressing activity. Noteworthily, BiP has been proven as an intracellular sensor of heavy metals.[90−93] Such feature possibly contributed to its sensitivity toward metallodrugs, so future designs of ICD compounds could use the scaffolds of **1a** and other known ICD metal agents as the leads to start with. As the binding interaction of metal complexes with biomolecular targets could be systematically tuned by the ligand design,[94,95] it is envisioned that metal complexes could be developed as potent ICD inducers with high specificity and robust efficacy. Besides the rational design, high-throughput screenings using a wide range of small molecules against BiP (either blocking its expression or enzymatic activity) may also contribute to the discovery of novel ICD agents.

ASSOCIATED CONTENT

Supporting Information

The Supporting Information is available free of charge at https://pubs.acs.org/doi/10.1021/jacs.2c02435.

Experimental procedures, synthesis steps, and analysis data of **Probe-Ir**; detection of the DAMP signal and Ser51 P-eIF2α of ICD in HCT116 cells; detection of the subcellular localization of PERK in HCT-8 cells; acute toxicity of **1a** measured in mice; streptavidin−HRP-based detection of biotinylated proteins; proteins identified in the LC−MS/MS detection of probe-Ir-enriched proteomes; native page gel of BiP; endogenous tryptophan fluorescence quenching of BiP; gene expression profiling of BiP in different cancer types of TCGA database; and correlation of BiP expression with patient survival in TCGA database (PDF)

AUTHOR INFORMATION

Corresponding Authors

Hong Liang − *State Key Laboratory for Chemistry and Molecular Engineering of Medicinal Resources, School of Chemistry & Pharmacy, Guangxi Normal University, Guilin, Guangxi 541004, P. R. China*; Email: hliang@gxnu.edu.cn

Taotao Zou − *Guangdong Key Laboratory of Chiral Molecule and Drug Discovery, School of Pharmaceutical Sciences, Sun Yat-Sen University, Guangzhou 510006, P. R. China*; orcid.org/0000-0001-9129-4398; Email: zoutt3@mail.sysu.edu.cn

Authors

Xiaolin Xiong − *Guangdong Key Laboratory of Chiral Molecule and Drug Discovery, School of Pharmaceutical Sciences, Sun Yat-Sen University, Guangzhou 510006, P. R. China*

Ke-Bin Huang − *State Key Laboratory for Chemistry and Molecular Engineering of Medicinal Resources, School of Chemistry & Pharmacy, Guangxi Normal University, Guilin, Guangxi 541004, P. R. China*; orcid.org/0000-0003-4773-4442

Yuan Wang − *Guangdong Key Laboratory of Chiral Molecule and Drug Discovery, School of Pharmaceutical Sciences, Sun Yat-Sen University, Guangzhou 510006, P. R. China*

Bei Cao − *Warshel Institute for Computational Biology, and General Education Division, The Chinese University of Hong Kong, Shenzhen 518172, P. R. China*

Yunli Luo − *Guangdong Key Laboratory of Chiral Molecule and Drug Discovery, School of Pharmaceutical Sciences, Sun Yat-Sen University, Guangzhou 510006, P. R. China*

Huowen Chen − *Guangdong Key Laboratory of Chiral Molecule and Drug Discovery, School of Pharmaceutical Sciences, Sun Yat-Sen University, Guangzhou 510006, P. R. China*

Yan Yang − *Guangdong Key Laboratory of Chiral Molecule and Drug Discovery, School of Pharmaceutical Sciences, Sun Yat-Sen University, Guangzhou 510006, P. R. China*

Yan Long − *Guangdong Key Laboratory of Chiral Molecule and Drug Discovery, School of Pharmaceutical Sciences, Sun Yat-Sen University, Guangzhou 510006, P. R. China*; Present Address: Pharmacy Department, The Seventh Affiliated Hospital of Sun Yat-Sen University, Shenzhen 518107, P. R. China

Moyi Liu − *Guangdong Key Laboratory of Chiral Molecule and Drug Discovery, School of Pharmaceutical Sciences, Sun Yat-Sen University, Guangzhou 510006, P. R. China*

Albert S. C. Chan − *Guangdong Key Laboratory of Chiral Molecule and Drug Discovery, School of Pharmaceutical Sciences, Sun Yat-Sen University, Guangzhou 510006, P. R. China*; orcid.org/0000-0003-1583-8503

Complete contact information is available at: https://pubs.acs.org/10.1021/jacs.2c02435

Author Contributions

[‖]X.X., K.-B.H., and Y.W. contributed equally.

Funding

This work was finically supported by the National Natural Science Foundation of China (nos. 22122706 and 32100058), China Postdoctoral Science Foundation (2021M703674), Guangdong Science and Technology Department (no. 2019QN01C125), Guangdong Basic and Applied Basic Research Foundation (nos. 2021A1515012347, 2021A1515011168, and 2020A1515110508), Guangzhou Science and Technology Projects (no. 202102020790), and Guangdong Provincial Key Lab of Chiral Molecule and Drug Discovery (no. 2019B030301005).

Notes

The authors declare no competing financial interest.

■ ACKNOWLEDGMENTS

This work is dedicated to Prof. Chi-Ming Che on the occasion of his 65th birthday. We sincerely thank Prof. Guohui Wan and Yuan Deng for their help in the measurement of acute toxicity of **1a** and Eric Snapp for kindly providing plasmids (BiP−mCherry).

■ ABBREVIATIONS

ICD	immunogenic cell death
ER	endoplasmic reticulum
BiP	binding immunoglobulin protein
DAMPs	damage-associated molecular patterns

■ REFERENCES

(1) Kroemer, G.; Galassi, C.; Zitvogel, L.; Galluzzi, L. Immunogenic cell stress and death. *Nat. Immunol.* **2022**, *23*, 487−500.
(2) Cella, M.; Sallusto, F.; Lanzavecchia, A. Origin, maturation and antigen presenting function of dendritic cells. *Curr. Opin. Immunol.* **1997**, *9*, 10−16.
(3) Aaes, T. L.; Kaczmarek, A.; Delvaeye, T.; De Craene, B.; De Koker, S.; Heyndrickx, L.; Delrue, I.; Taminau, J.; Wiernicki, B.; De Groote, P.; Garg, A. D.; Leybaert, L.; Grooten, J.; Bertrand, M. J. M.; Agostinis, P.; Berx, G.; Declercq, W.; Vandenabeele, P.; Krysko, D. V. Vaccination with Necroptotic Cancer Cells Induces Efficient Anti-tumor Immunity. *Cell Rep.* **2016**, *15*, 274−287.
(4) Zhang, Z.; Zhang, Y.; Xia, S.; Kong, Q.; Li, S.; Liu, X.; Junqueira, C.; Meza-Sosa, K. F.; Mok, T. M. Y.; Ansara, J.; Sengupta, S.; Yao, Y.; Wu, H.; Lieberman, J. Gasdermin E suppresses tumour growth by activating anti-tumour immunity. *Nature* **2020**, *579*, 415−420.
(5) Panaretakis, T.; Kepp, O.; Brockmeier, U.; Tesniere, A.; Bjorklund, A.-C.; Chapman, D. C.; Durchschlag, M.; Joza, N.; Pierron, G.; van Endert, P.; Yuan, J.; Zitvogel, L.; Madeo, F.; Williams, D. B.; Kroemer, G. Mechanisms of pre-apoptotic calreticulin exposure in immunogenic cell death. *EMBO J.* **2009**, *28*, 578−590.
(6) Fucikova, J.; Kepp, O.; Kasikova, L.; Petroni, G.; Yamazaki, T.; Liu, P.; Zhao, L.; Spisek, R.; Kroemer, G.; Galluzzi, L. Detection of immunogenic cell death and its relevance for cancer therapy. *Cell Death Dis.* **2020**, *11*, 1013.
(7) Rivera Vargas, T.; Apetoh, L. Danger signals: Chemotherapy enhancers? *Immunol. Rev.* **2017**, *280*, 175−193.
(8) Limagne, E.; Thibaudin, M.; Nuttin, L.; Spill, A.; Derangère, V.; Fumet, J.-D.; Amellal, N.; Peranzoni, E.; Cattan, V.; Ghiringhelli, F. Trifluridine/Tipiracil plus Oxaliplatin Improves PD-1 Blockade in Colorectal Cancer by Inducing Immunogenic Cell Death and Depleting Macrophages. *Cancer Immunol. Res.* **2019**, *7*, 1958−1969.
(9) Yu, J.; He, X.; Wang, Z.; Wang, Y.; Liu, S.; Li, X.; Huang, Y. Combining PD-L1 inhibitors with immunogenic cell death triggered by chemo-photothermal therapy via a thermosensitive liposome system to stimulate tumor-specific immunological response. *Nanoscale* **2021**, *13*, 12966−12978.
(10) Kepp, O.; Zitvogel, L.; Kroemer, G. Clinical evidence that immunogenic cell death sensitizes to PD-1/PD-L1 blockade. *Oncoimmunology* **2019**, *8*, No. e1637188.
(11) Srivastava, S.; Furlan, S. N.; Jaeger-Ruckstuhl, C. A.; Sarvothama, M.; Berger, C.; Smythe, K. S.; Garrison, S. M.; Specht, J. M.; Lee, S. M.; Amezquita, R. A.; Voillet, V.; Muhunthan, V.; Yechan-Gunja, S.; Pillai, S. P. S.; Rader, C.; Houghton, A. M.; Pierce, R. H.; Gottardo, R.; Maloney, D. G.; Riddell, S. R. Immunogenic Chemotherapy Enhances Recruitment of CAR-T Cells to Lung Tumors and Improves Antitumor Efficacy when Combined with Checkpoint Blockade. *Cancer Cell* **2021**, *39*, 193−208.e10.
(12) Wang, Q.; Ju, X.; Wang, J.; Fan, Y.; Ren, M.; Zhang, H. Immunogenic cell death in anticancer chemotherapy and its impact on clinical studies. *Cancer Lett.* **2018**, *438*, 17−23.
(13) Vanmeerbeek, I.; Sprooten, J.; De Ruysscher, D.; Tejpar, S.; Vandenberghe, P.; Fucikova, J.; Spisek, R.; Zitvogel, L.; Kroemer, G.; Galluzzi, L.; Garg, A. D. Trial watch: chemotherapy-induced immunogenic cell death in immuno-oncology. *Oncoimmunology* **2020**, *9*, 1703449.
(14) Casares, N.; Pequignot, M. O.; Tesniere, A.; Ghiringhelli, F.; Roux, S.; Chaput, N.; Schmitt, E.; Hamai, A.; Hervas-Stubbs, S.; Obeid, M.; Coutant, F.; Metivier, D.; Pichard, E.; Aucouturier, P.; Pierron, G.; Garrido, C.; Zitvogel, L.; Kroemer, G. Caspase-dependent immunogenicity of doxorubicin-induced tumor cell death. *J. Exp. Med.* **2005**, *202*, 1691−1701.
(15) Zhou, J.; Wang, G.; Chen, Y.; Wang, H.; Hua, Y.; Cai, Z. Immunogenic cell death in cancer therapy: Present and emerging inducers. *J. Cell. Mol. Med.* **2019**, *23*, 4854−4865.
(16) Terenzi, A.; Pirker, C.; Keppler, B. K.; Berger, W. Anticancer metal drugs and immunogenic cell death. *J. Inorg. Biochem.* **2016**, *165*, 71−79.
(17) Sen, S.; Won, M.; Levine, M. S.; Noh, Y.; Sedgwick, A. C.; Kim, J. S.; Sessler, J. L.; Arambula, J. F. Metal-based anticancer agents as immunogenic cell death inducers: the past, present, and future. *Chem. Soc. Rev.* **2022**, *51*, 1212−1233.
(18) Englinger, B.; Pirker, C.; Heffeter, P.; Terenzi, A.; Kowol, C. R.; Keppler, B. K.; Berger, W. Metal Drugs and the Anticancer Immune Response. *Chem. Rev.* **2019**, *119*, 1519−1624.
(19) Huang, K.-B.; Wang, F.-Y.; Feng, H.-W.; Luo, H.; Long, Y.; Zou, T.; Chan, A. S. C.; Liu, R.; Zou, H.; Chen, Z.-F.; Liu, Y.-C.; Liu, Y.-N.; Liang, H. An aminophosphonate ester ligand-containing platinum(ii) complex induces potent immunogenic cell death in vitro and elicits effective anti-tumour immune responses in vivo. *Chem. Commun.* **2019**, *55*, 13066−13069.
(20) Sabbatini, M.; Zanellato, I.; Ravera, M.; Gabano, E.; Perin, E.; Rangone, B.; Osella, D. Pt(IV) Bifunctional Prodrug Containing 2-(2-Propynyl)octanoato Axial Ligand: Induction of Immunogenic Cell Death on Colon Cancer. *J. Med. Chem.* **2019**, *62*, 3395−3406.
(21) Sun, Y.; Yin, E.; Tan, Y.; Yang, T.; Song, D.; Jin, S.; Guo, Z.; Wang, X. Immunogenicity and cytotoxicity of a platinum(IV) complex derived from capsaicin. *Dalton Trans.* **2021**, *50*, 3516−3522.
(22) Novohradsky, V.; Markova, L.; Kostrhunova, H.; Kasparkova, J.; Hoeschele, J.; Brabec, V. A [Pt(cis-1,3-diaminocycloalkane)Cl2] analog exhibits hallmarks typical of immunogenic cell death inducers in model cancer cells. *J. Inorg. Biochem.* **2022**, *226*, 111628.
(23) Tham, M. J. R.; Babak, M. V.; Ang, W. H. PlatinER: a Highly Potent Anticancer Platinum(II) Complex that induces Endoplasmic Reticulum Stress-driven Immunogenic Cell Death. *Angew. Chem., Int. Ed.* **2020**, *59*, 19070−19078.
(24) Yamazaki, T.; Buqué, A.; Ames, T. D.; Galluzzi, L. PT-112 induces immunogenic cell death and synergizes with immune checkpoint blockers in mouse tumor models. *Oncoimmunology* **2020**, *9*, 1721810.
(25) Novohradsky, V.; Pracharova, J.; Kasparkova, J.; Imberti, C.; Bridgewater, H. E.; Sadler, P. J.; Brabec, V. Induction of immunogenic cell death in cancer cells by a photoactivated platinum(IV) prodrug. *Inorg. Chem. Front.* **2020**, *7*, 4150−4159.
(26) Wong, D. Y. Q.; Ong, W. W. F.; Ang, W. H. Induction of immunogenic cell death by chemotherapeutic platinum complexes. *Angew. Chem., Int. Ed.* **2015**, *54*, 6483−6487.
(27) Groer, C.; Zhang, T.; Lu, R.; Cai, S.; Mull, D.; Huang, A.; Forrest, M.; Berkland, C.; Aires, D.; Forrest, M. L. Intratumoral Cancer Chemotherapy with a Carrier-Based Immunogenic Cell-Death Eliciting Platinum (IV) Agent. *Mol. Pharm.* **2020**, *17*, 4334−4345.
(28) Deng, Z.; Wang, N.; Liu, Y.; Xu, Z.; Wang, Z.; Lau, T.-C.; Zhu, G. A Photocaged, Water-Oxidizing, and Nucleolus-Targeted Pt(IV) Complex with a Distinct Anticancer Mechanism. *J. Am. Chem. Soc.* **2020**, *142*, 7803−7812.
(29) Wong, D. Y. Q.; Yeo, C. H. F.; Ang, W. H. Immuno-chemotherapeutic platinum(IV) prodrugs of cisplatin as multimodal anticancer agents. *Angew. Chem., Int. Ed.* **2014**, *53*, 6752−6756.
(30) Bian, M.; Fan, R.; Yang, Z.; Chen, Y.; Xu, Z.; Lu, Y.; Liu, W. Pt(II)-NHC Complex Induces ROS-ERS-Related DAMP Balance to

Harness Immunogenic Cell Death in Hepatocellular Carcinoma. *J. Med. Chem.* **2022**, *65*, 1848−1866.
(31) Wernitznig, D.; Kiakos, K.; Del Favero, G.; Harrer, N.; Machat, H.; Osswald, A.; Jakupec, M. A.; Wernitznig, A.; Sommergruber, W.; Keppler, B. K. First-in-class ruthenium anticancer drug (KP1339/IT-139) induces an immunogenic cell death signature in colorectal spheroids in vitro. *Metallomics* **2019**, *11*, 1044−1048.
(32) Konda, P.; Lifshits, L. M.; Roque, J. A., 3rd; Cole, H. D.; Cameron, C. G.; McFarland, S. A.; Gujar, S. Discovery of immunogenic cell death-inducing ruthenium-based photosensitizers for anticancer photodynamic therapy. *Oncoimmunology* **2020**, *10*, 1863626.
(33) Wernitznig, D.; Meier-Menches, S. M.; Cseh, K.; Theiner, S.; Wenisch, D.; Schweikert, A.; Jakupec, M. A.; Koellensperger, G.; Wernitznig, A.; Sommergruber, W.; Keppler, B. K. Plecstatin-1 induces an immunogenic cell death signature in colorectal tumour spheroids. *Metallomics* **2020**, *12*, 2121−2133.
(34) Su, X.; Wang, W. J.; Cao, Q.; Zhang, H.; Liu, B.; Ling, Y.; Zhou, X.; Mao, Z. W. A Carbonic Anhydrase IX (CAIX)-Anchored Rhenium(I) Photosensitizer Evokes Pyroptosis for Enhanced Anti-Tumor Immunity. *Angew. Chem., Int. Ed.* **2022**, *61*, No. e202115800.
(35) Le, H. V.; Babak, M. V.; Ehsan, M. A.; Altaf, M.; Reichert, L.; Gushchin, A. L.; Ang, W. H.; Isab, A. A. Highly cytotoxic gold(i)-phosphane dithiocarbamate complexes trigger an ER stress-dependent immune response in ovarian cancer cells. *Dalton Trans.* **2020**, *49*, 7355−7363.
(36) Sen, S.; Hufnagel, S.; Maier, E. Y.; Aguilar, I.; Selvakumar, J.; DeVore, J. E.; Lynch, V. M.; Arumugam, K.; Cui, Z.; Sessler, J. L.; Arambula, J. F. Rationally Designed Redox-Active Au(I) N-Heterocyclic Carbene: An Immunogenic Cell Death Inducer. *J. Am. Chem. Soc.* **2020**, *142*, 20536−20541.
(37) Ji, S.; Yang, X.; Chen, X.; Li, A.; Yan, D.; Xu, H.; Fei, H. Structure-tuned membrane active Ir-complexed oligoarginine overcomes cancer cell drug resistance and triggers immune responses in mice. *Chem. Sci.* **2020**, *11*, 9126−9133.
(38) Wang, L.; Guan, R.; Xie, L.; Liao, X.; Xiong, K.; Rees, T. W.; Chen, Y.; Ji, L.; Chao, H. An ER-Targeting Iridium(III) Complex That Induces Immunogenic Cell Death in Non-Small-Cell Lung Cancer. *Angew. Chem., Int. Ed.* **2021**, *60*, 4657−4665.
(39) Vigueras, G.; Markova, L.; Novohradsky, V.; Marco, A.; Cutillas, N.; Kostrhunova, H.; Kasparkova, J.; Ruiz, J.; Brabec, V. A photoactivated Ir(iii) complex targets cancer stem cells and induces secretion of damage-associated molecular patterns in melanoma cells characteristic of immunogenic cell death. *Inorg. Chem. Front.* **2021**, *8*, 4696−4711.
(40) Wang, F.-X.; Liu, J.-W.; Hong, X.-Q.; Tan, C.-P.; Zhang, L.; Chen, W.-H.; Sadler, P. J.; Mao, Z.-W. Anion-Responsive Manganese Porphyrin Facilitates Chloride Transport and Induces Immunogenic Cell Death. *CCS Chem.* **2021**, *3*, 2527−2537.
(41) Kaur, P.; Johnson, A.; Northcote-Smith, J.; Lu, C.; Suntharalingam, K. Immunogenic Cell Death of Breast Cancer Stem Cells Induced by an Endoplasmic Reticulum-Targeting Copper(II) Complex. *ChemBioChem* **2020**, *21*, 3618−3624.
(42) Flieswasser, T.; Van Loenhout, J.; Freire Boullosa, L.; Van den Eynde, A.; De Waele, J.; Van Audenaerde, J.; Lardon, F.; Smits, E.; Pauwels, P.; Jacobs, J. Clinically Relevant Chemotherapeutics Have the Ability to Induce Immunogenic Cell Death in Non-Small Cell Lung Cancer. *Cells* **2020**, *9*, 1474.
(43) Kepp, O.; Menger, L.; Vacchelli, E.; Locher, C.; Adjemian, S.; Yamazaki, T.; Martins, I.; Sukkurwala, A. Q.; Michaud, M.; Senovilla, L.; Galluzzi, L.; Kroemer, G.; Zitvogel, L. Crosstalk between ER stress and immunogenic cell death. *Cytokine Growth Factor Rev.* **2013**, *24*, 311−318.
(44) King, A. P.; Wilson, J. J. Endoplasmic reticulum stress: an arising target for metal-based anticancer agents. *Chem. Soc. Rev.* **2020**, *49*, 8113−8136.
(45) Li, Y.; Tan, C.-P.; Zhang, W.; He, L.; Ji, L.-N.; Mao, Z.-W. Phosphorescent iridium(III)-bis-N-heterocyclic carbene complexes as mitochondria-targeted theranostic and photodynamic anticancer agents. *Biomaterials* **2015**, *39*, 95−104.
(46) Yang, C.; Mehmood, F.; Lam, T. L.; Chan, S. L.-F.; Wu, Y.; Yeung, C.-S.; Guan, X.; Li, K.; Chung, C. Y.-S.; Zhou, C.-Y.; Zou, T.; Che, C.-M. Stable luminescent iridium(iii) complexes with bis(N-heterocyclic carbene) ligands: photo-stability, excited state properties, visible-light-driven radical cyclization and CO2 reduction, and cellular imaging. *Chem. Sci.* **2016**, *7*, 3123−3136.
(47) Schindelin, J.; Arganda-Carreras, I.; Frise, E.; Kaynig, V.; Longair, M.; Pietzsch, T.; Preibisch, S.; Rueden, C.; Saalfeld, S.; Schmid, B.; Tinevez, J.-Y.; White, D. J.; Hartenstein, V.; Eliceiri, K.; Tomancak, P.; Cardona, A. Fiji: an open-source platform for biological-image analysis. *Nat. Methods* **2012**, *9*, 676−682.
(48) Obeid, M.; Tesniere, A.; Ghiringhelli, F.; Fimia, G. M.; Apetoh, L.; Perfettini, J.-L.; Castedo, M.; Mignot, G.; Panaretakis, T.; Casares, N.; Métivier, D.; Larochette, N.; van Endert, P.; Ciccosanti, F.; Piacentini, M.; Zitvogel, L.; Kroemer, G. Calreticulin exposure dictates the immunogenicity of cancer cell death. *Nat. Med.* **2007**, *13*, 54−61.
(49) Gardai, S. J.; McPhillips, K. A.; Frasch, S. C.; Janssen, W. J.; Starefeldt, A.; Murphy-Ullrich, J. E.; Bratton, D. L.; Oldenborg, P.-A.; Michalak, M.; Henson, P. M. Cell-surface calreticulin initiates clearance of viable or apoptotic cells through trans-activation of LRP on the phagocyte. *Cell* **2005**, *123*, 321−334.
(50) Bezu, L.; Sauvat, A.; Humeau, J.; Gomes-da-Silva, L. C.; Iribarren, K.; Forveille, S.; Garcia, P.; Zhao, L.; Liu, P.; Zitvogel, L.; Senovilla, L.; Kepp, O.; Kroemer, G. eIF2alpha phosphorylation is pathognomonic for immunogenic cell death. *Cell Death Differ.* **2018**, *25*, 1375−1393.
(51) Bezu, L.; Sauvat, A.; Humeau, J.; Leduc, M.; Kepp, O.; Kroemer, G. eIF2alpha phosphorylation: A hallmark of immunogenic cell death. *Oncoimmunology* **2018**, *7*, No. e1431089.
(52) Kepp, O.; Senovilla, L.; Vitale, I.; Vacchelli, E.; Adjemian, S.; Agostinis, P.; Apetoh, L.; Aranda, F.; Barnaba, V.; Bloy, N.; Bracci, L.; Breckpot, K.; Brough, D.; Buqué, A.; Castro, M. G.; Cirone, M.; Colombo, M. I.; Cremer, I.; Demaria, S.; Dini, L.; Eliopoulos, A. G.; Faggioni, A.; Formenti, S. C.; Fučíková, J.; Gabriele, L.; Gaipl, U. S.; Galon, J.; Garg, A.; Ghiringhelli, F.; Giese, N. A.; Guo, Z. S.; Hemminki, A.; Herrmann, M.; Hodge, J. W.; Holdenrieder, S.; Honeychurch, J.; Hu, H.-M.; Huang, X.; Illidge, T. M.; Kono, K.; Korbelik, M.; Krysko, D. V.; Loi, S.; Lowenstein, P. R.; Lugli, E.; Ma, Y.; Madeo, F.; Manfredi, A. A.; Martins, I.; Mavilio, D.; Menger, L.; Merendino, N.; Michaud, M.; Mignot, G.; Mossman, K. L.; Multhoff, G.; Oehler, R.; Palombo, F.; Panaretakis, T.; Pol, J.; Proietti, E.; Ricci, J.-E.; Riganti, C.; Rovere-Querini, P.; Rubartelli, A.; Sistigu, A.; Smyth, M. J.; Sonnemann, J.; Spisek, R.; Stagg, J.; Sukkurwala, A. Q.; Tartour, E.; Thorburn, A.; Thorne, S. H.; Vandenabeele, P.; Velotti, F.; Workenhe, S. T.; Yang, H.; Zong, W.-X.; Zitvogel, L.; Kroemer, G.; Galluzzi, L. Consensus guidelines for the detection of immunogenic cell death. *Oncoimmunology* **2014**, *3*, No. e955691.
(53) Galluzzi, L.; Vitale, I.; Warren, S.; Adjemian, S.; Agostinis, P.; Martinez, A. B.; Chan, T. A.; Coukos, G.; Demaria, S.; Deutsch, E.; Draganov, D.; Edelson, R. L.; Formenti, S. C.; Fucikova, J.; Gabriele, L.; Gaipl, U. S.; Gameiro, S. R.; Garg, A. D.; Golden, E.; Han, J.; Harrington, K. J.; Hemminki, A.; Hodge, J. W.; Hossain, D. M. S.; Illidge, T.; Karin, M.; Kaufman, H. L.; Kepp, O.; Kroemer, G.; Lasarte, J. J.; Loi, S.; Lotze, M. T.; Manic, G.; Merghoub, T.; Melcher, A. A.; Mossman, K. L.; Prosper, F.; Rekdal, Ø.; Rescigno, M.; Riganti, C.; Sistigu, A.; Smyth, M. J.; Spisek, R.; Stagg, J.; Strauss, B. E.; Tang, D.; Tatsuno, K.; van Gool, S. W.; Vandenabeele, P.; Yamazaki, T.; Zamarin, D.; Zitvogel, L.; Cesano, A.; Marincola, F. M. Consensus guidelines for the definition, detection and interpretation of immunogenic cell death. *J. Immunother. Cancer* **2020**, *8*, No. e000337.
(54) Ha, J.; Park, H.; Park, J.; Park, S. B. Recent advances in identifying protein targets in drug discovery. *Cell Chem. Biol.* **2021**, *28*, 394−423.
(55) Farrer, N. J.; Griffith, D. M. Exploiting azide-alkyne click chemistry in the synthesis, tracking and targeting of platinum anticancer complexes. *Curr. Opin. Chem. Biol.* **2020**, *55*, 59−68.

(56) Fung, S. K.; Zou, T.; Cao, B.; Lee, P.-Y.; Fung, Y. M. E.; Hu, D.; Lok, C.-N.; Che, C.-M. Cyclometalated Gold(III) Complexes Containing N-Heterocyclic Carbene Ligands Engage Multiple Anti-Cancer Molecular Targets. *Angew. Chem., Int. Ed.* **2017**, *56*, 3892−3896.
(57) Wang, H.; Zhou, Y.; Xu, X.; Li, H.; Sun, H. Metalloproteomics in conjunction with other omics for uncovering the mechanism of action of metallodrugs: Mechanism-driven new therapy development. *Curr. Opin. Chem. Biol.* **2020**, *55*, 171−179.
(58) Hu, D.; Liu, Y.; Lai, Y.-T.; Tong, K.-C.; Fung, Y.-M.; Lok, C.-N.; Che, C.-M. Anticancer Gold(III) Porphyrins Target Mitochondrial Chaperone Hsp60. *Angew. Chem., Int. Ed.* **2016**, *55*, 1387−1391.
(59) Szklarczyk, D.; Gable, A. L.; Nastou, K. C.; Lyon, D.; Kirsch, R.; Pyysalo, S.; Doncheva, N. T.; Legeay, M.; Fang, T.; Bork, P.; Jensen, L. J.; von Mering, C. The STRING database in 2021: customizable protein-protein networks, and functional characterization of user-uploaded gene/measurement sets. *Nucleic Acids Res.* **2021**, *49*, D605−D612.
(60) Chen, X.; Cubillos-Ruiz, J. R. Endoplasmic reticulum stress signals in the tumour and its microenvironment. *Nat. Rev. Cancer* **2021**, *21*, 71−88.
(61) Korennykh, A.; Walter, P. Structural basis of the unfolded protein response. *Annu. Rev. Cell Dev. Biol.* **2012**, *28*, 251−277.
(62) Vitale, M.; Bakunts, A.; Orsi, A.; Lari, F.; Tade, L.; Danieli, A.; Rato, C.; Valetti, C.; Sitia, R.; Raimondi, A.; Christianson, J. C.; van Anken, E. Inadequate BiP availability defines endoplasmic reticulum stress. *Elife* **2019**, *8*, No. e41168.
(63) Lai, C. W.; Aronson, D. E.; Snapp, E. L. BiP availability distinguishes states of homeostasis and stress in the endoplasmic reticulum of living cells. *Mol. Biol. Cell* **2010**, *21*, 1909−1921.
(64) Molina, D. M.; Jafari, R.; Ignatushchenko, M.; Seki, T.; Larsson, E. A.; Dan, C.; Sreekumar, L.; Cao, Y.; Nordlund, P. Monitoring drug target engagement in cells and tissues using the cellular thermal shift assay. *Science* **2013**, *341*, 84−87.
(65) Hu, D.; Yang, C.; Lok, C. N.; Xing, F.; Lee, P. Y.; Fung, Y. M. E.; Jiang, H.; Che, C. M. An Antitumor Bis(N-Heterocyclic Carbene)Platinum(II) Complex That Engages Asparagine Synthetase as an Anticancer Target. *Angew. Chem., Int. Ed.* **2019**, *58*, 10914−10918.
(66) Wang, Y.; Hu, L.; Xu, F.; Quan, Q.; Lai, Y.-T.; Xia, W.; Yang, Y.; Chang, Y.-Y.; Yang, X.; Chai, Z.; Wang, J.; Chu, I. K.; Li, H.; Sun, H. Integrative approach for the analysis of the proteome-wide response to bismuth drugs in Helicobacter pylori. *Chem. Sci.* **2017**, *8*, 4626−4633.
(67) Wang, H.; Wang, M.; Yang, X.; Xu, X.; Hao, Q.; Yan, A.; Hu, M.; Lobinski, R.; Li, H.; Sun, H. Antimicrobial silver targets glyceraldehyde-3-phosphate dehydrogenase in glycolysis of E. coli. *Chem. Sci.* **2019**, *10*, 7193−7199.
(68) Kopp, M. C.; Larburu, N.; Durairaj, V.; Adams, C. J.; Ali, M. M. U. UPR proteins IRE1 and PERK switch BiP from chaperone to ER stress sensor. *Nat. Struct. Mol. Biol.* **2019**, *26*, 1053−1062.
(69) Carrara, M.; Prischi, F.; Nowak, P. R.; Kopp, M. C.; Ali, M. M. Noncanonical binding of BiP ATPase domain to Ire1 and Perk is dissociated by unfolded protein CH1 to initiate ER stress signaling. *Elife* **2015**, *4*, No. e03522.
(70) Cerezo, M.; Lehraiki, A.; Millet, A.; Rouaud, F.; Plaisant, M.; Jaune, E.; Botton, T.; Ronco, C.; Abbe, P.; Amdouni, H.; Passeron, T.; Hofman, V.; Mograbi, B.; Dabert-Gay, A.-S.; Debayle, D.; Alcor, D.; Rabhi, N.; Annicotte, J.-S.; Héliot, L.; Gonzalez-Pisfil, M.; Robert, C.; Moréra, S.; Vigouroux, A.; Gual, P.; Ali, M. M. U.; Bertolotto, C.; Hofman, P.; Ballotti, R.; Benhida, R.; Rocchi, S. Compounds Triggering ER Stress Exert Anti-Melanoma Effects and Overcome BRAF Inhibitor Resistance. *Cancer Cell* **2016**, *29*, 805−819.
(71) Burris, H. A.; Bakewell, S.; Bendell, J. C.; Infante, J.; Jones, S. F.; Spigel, D. R.; Weiss, G. J.; Ramanathan, R. K.; Ogden, A.; Von Hoff, D. Safety and activity of IT-139, a ruthenium-based compound, in patients with advanced solid tumours: a first-in-human, open-label, dose-escalation phase I study with expansion cohort. *ESMO Open* **2016**, *1*, No. e000154.
(72) Bakewell, S. J.; Rangel, D. F.; Ha, D. P.; Sethuraman, J.; Crouse, R.; Hadley, E.; Costich, T. L.; Zhou, X.; Nichols, P.; Lee, A. S. Suppression of stress induction of the 78-kilodalton glucose regulated protein (GRP78) in cancer by IT-139, an anti-tumor ruthenium small molecule inhibitor. *Oncotarget* **2018**, *9*, 29698−29714.
(73) Schoenhacker-Alte, B.; Mohr, T.; Pirker, C.; Kryeziu, K.; Kuhn, P.-S.; Buck, A.; Hofmann, T.; Gerner, C.; Hermann, G.; Koellensperger, G.; Keppler, B. K.; Berger, W.; Heffeter, P. Sensitivity towards the GRP78 inhibitor KP1339/IT-139 is characterized by apoptosis induction via caspase 8 upon disruption of ER homeostasis. *Cancer Lett.* **2017**, *404*, 79−88.
(74) Flocke, L. S.; Trondl, R.; Jakupec, M. A.; Keppler, B. K. Molecular mode of action of NKP-1339-a clinically investigated ruthenium-based drug-involves ER- and ROS-related effects in colon carcinoma cell lines. *Invest. New Drugs* **2016**, *34*, 261−268.
(75) Neuditschko, B.; Legin, A. A.; Baier, D.; Schintlmeister, A.; Reipert, S.; Wagner, M.; Keppler, B. K.; Berger, W.; Meier-Menches, S. M.; Gerner, C. Interaction with Ribosomal Proteins Accompanies Stress Induction of the Anticancer Metallodrug BOLD-100/KP1339 in the Endoplasmic Reticulum. *Angew. Chem., Int. Ed.* **2021**, *60*, 5063−5068.
(76) Todd, R. C.; Lippard, S. J. Inhibition of transcription by platinum antitumor compounds. *Metallomics* **2009**, *1*, 280−291.
(77) Ang, W. H.; Myint, M.; Lippard, S. J. Transcription inhibition by platinum-DNA cross-links in live mammalian cells. *J. Am. Chem. Soc.* **2010**, *132*, 7429−7435.
(78) Gniazdowski, M.; Denny, W.; Nelson, S.; Czyz, M. Transcription factors as targets for DNA-interacting drugs. *Curr. Med. Chem.* **2003**, *10*, 909−924.
(79) Humeau, J.; Sauvat, A.; Cerrato, G.; Xie, W.; Loos, F.; Iannantuoni, F.; Bezu, L.; Lévesque, S.; Paillet, J.; Pol, J.; Leduc, M.; Zitvogel, L.; de Thé, H.; Kepp, O.; Kroemer, G. Inhibition of transcription by dactinomycin reveals a new characteristic of immunogenic cell stress. *EMBO Mol. Med.* **2020**, *12*, No. e11622.
(80) Rao, R. V.; Peel, A.; Logvinova, A.; del Rio, G.; Hermel, E.; Yokota, T.; Goldsmith, P. C.; Ellerby, L. M.; Ellerby, H. M.; Bredesen, D. E. Coupling endoplasmic reticulum stress to the cell death program: role of the ER chaperone GRP78. *FEBS Lett.* **2002**, *514*, 122−128.
(81) Tang, Z.; Kang, B.; Li, C.; Chen, T.; Zhang, Z. GEPIA2: an enhanced web server for large-scale expression profiling and interactive analysis. *Nucleic Acids Res.* **2019**, *47*, W556−W560.
(82) Pyrko, P.; Schönthal, A. H.; Hofman, F. M.; Chen, T. C.; Lee, A. S. The unfolded protein response regulator GRP78/BiP as a novel target for increasing chemosensitivity in malignant gliomas. *Cancer Res.* **2007**, *67*, 9809−9816.
(83) Zhu, X.; Zhang, Y.; Luo, Q.; Wu, X.; Huang, F.; Shu, T.; Wan, Y.; Chen, H.; Liu, Z. The deubiquitinase USP11 promotes ovarian cancer chemoresistance by stabilizing BIP. *Signal Transduction Targeted Ther.* **2021**, *6*, 264.
(84) Gifford, J. B.; Huang, W.; Zeleniak, A. E.; Hindoyan, A.; Wu, H.; Donahue, T. R.; Hill, R. Expression of GRP78, Master Regulator of the Unfolded Protein Response, Increases Chemoresistance in Pancreatic Ductal Adenocarcinoma. *Mol. Cancer Ther.* **2016**, *15*, 1043−1052.
(85) Lee, A. S. Glucose regulated proteins in cancer: molecular mechanisms and therapeutic potential. *Nat. Rev. Cancer* **2014**, *14*, 263−276.
(86) Yang, W.; Xiu, Z.; He, Y.; Huang, W.; Li, Y.; Sun, T. Bip inhibition in glioma stem cells promotes radiation-induced immunogenic cell death. *Cell Death Dis.* **2020**, *11*, 786.
(87) Huang, K. C. Y.; Chiang, S. F.; Yang, P. C.; Ke, T. W.; Chen, T. W.; Lin, C. Y.; Chang, H. Y.; Chen, W. T. L.; Chao, K. S. C. ATAD3A stabilizes GRP78 to suppress ER stress for acquired chemoresistance in colorectal cancer. *J. Cell. Physiol.* **2021**, *236*, 6481−6495.
(88) Krysko, D. V.; Garg, A. D.; Kaczmarek, A.; Krysko, O.; Agostinis, P.; Vandenabeele, P. Immunogenic cell death and DAMPs in cancer therapy. *Nat. Rev. Cancer* **2012**, *12*, 860−875.

https://doi.org/10.1021/jacs.2c02435
J. Am. Chem. Soc. 2022, 144, 10407−10416

(89) Garg, A. D.; Dudek-Peric, A. M.; Romano, E.; Agostinis, P. Immunogenic cell death. *Int. J. Dev. Biol.* **2015**, *59*, 131−140.
(90) Falahatpisheh, H.; Nanez, A.; Montoya-Durango, D.; Qian, Y.; Tiffany-Castiglioni, E.; Ramos, K. S. Activation profiles of HSPA5 during the glomerular mesangial cell stress response to chemical injury. *Cell Stress Chaperones* **2007**, *12*, 209−218.
(91) Wang, T.; Yuan, Y.; Zou, H.; Yang, J.; Zhao, S.; Ma, Y.; Wang, Y.; Bian, J.; Liu, X.; Gu, J.; Liu, Z.; Zhu, J. The ER stress regulator Bip mediates cadmium-induced autophagy and neuronal senescence. *Sci. Rep.* **2016**, *6*, 38091.
(92) Tiffany-Castiglioni, E.; Qian, Y.; Barhoumi, R.; Zheng, Y. Determination of metal interactions with the chaperone Hspa5 in human astrocytoma cells and rat astrocyte primary cultures. *Methods Mol. Biol.* **2011**, *758*, 29−48.
(93) Qian, Y.; Meng, B.; Zhang, X.; Zheng, Y.; Taylor, R.; Tiffany-Castiglioni, E. HSPA5 forms specific complexes with copper. *Neurochem. Res.* **2013**, *38*, 321−329.
(94) Marzo, T.; Ferraro, G.; Merlino, A.; Messori, L. Protein Metalation by Inorganic Anticancer Drugs. In *Encyclopedia of Inorganic and Bioinorganic Chemistry*; Scott, R. A., Ed.; John Wiley & Sons, Ltd., 2022.
(95) Anthony, E. J.; Bolitho, E. M.; Bridgewater, H. E.; Carter, O. W. L.; Donnelly, J. M.; Imberti, C.; Lant, E. C.; Lermyte, F.; Needham, R. J.; Palau, M.; Sadler, P. J.; Shi, H.; Wang, F.-X.; Zhang, W.-Y.; Zhang, Z. Metallodrugs are unique: opportunities and challenges of discovery and development. *Chem. Sci.* **2020**, *11*, 12888−12917.

https://doi.org/10.1021/jacs.2c02435
J. Am. Chem. Soc. 2022, 144, 10407−10416